The hydromechanical behaviour of unsaturated loess in slopes, New Zealand

Katherine Yates[1*], and *Adrian* Russell[2]

[1]Department of Civil and Natural Resources, University of Canterbury, Christchurch, New Zealand
[2]School of Civil and Environmental Engineering, The University of New South Wales, Sydney, Australia

Abstract. Unsaturated loess and loess-derived soils in the Akaroa harbour area of New Zealand are vulnerable to shallow landsliding during rainfall events. Laboratory testing and long-term field instrumentation has been conducted to characterise the water retention and unsaturated shear strength of these materials, and better understand temporal changings in slope stability. Laboratory test results indicate that the same soil-water characteristic curve can be applied to both recompacted and intact loess when suction is normalised by the air entry value. Conversely the stress-strain behaviours of the recompacted and intact loess were different due to the unique microstructure of the intact loess that contributes to its shear strength. Long-term field instrumentation data showed that, for the duration of the monitoring period, the hydraulic state of the loess remained on a scanning curve. These data, combined with the laboratory testing, confirm that temporal variation in slope stability can be attributed to seasonal variability in suction and its contribution to unsaturated shear strength. These hydromechanical variabilities, resulting from wetting and drying, are affected by rainfall intensity and duration that occurs at the site.

1 Introduction

Aeolian loess deposits cover 10 % of the South Island of New Zealand [1-5]. When unsaturated, these soils are stable in near vertical cut slopes and tend to exhibit a strength typical of weak rock [6, 7]. During rainfall, water infiltrates into the soil mass increasing the water content and decreasing suction leading to a reduction in shear strength and initiation of shallow slope instabilities. Previous research has identified a relationship between a shear strength reduction and an increase in water content and how that gives rise to slope instability [7-9]. However, these studies have not quantified the direct effect of suction on unsaturated shear strength and have predominantly focused on the behaviour of recompacted loess overlooking the contribution of intact microstructural to strength and hydromechanical properties.

Laboratory testing has been conducted to determine the soil-water characteristics of intact and recompacted unsaturated loess from Banks Peninsula, New Zealand. These data are presented alongside triaxial test results on saturated and unsaturated samples. Fractal properties of the loess are used to describe the soil-water characteristic curve [10-13]. In situ field instrumentation data shows how the hydraulic state of a natural loess slope changes when subject to climatic wetting and drying periods. These data indicate that hydraulic wetting occurs when rainfall intensity and duration are >1.5 mm/hr and 400min respectively.

2 Field instrumentation

The Akaroa Harbour region was selected for field instrumentation due to the frequent occurrence of rainfall-triggered slope failures and increasing demand for rural and residential development. In this region the loess is ≤ 30 m thick and covers Miocene age volcanic rock. Field instrumentation was installed across a ~ 95 m^2 sloped monitoring site in the Akaroa harbour region and used to examine the hydraulic response of loess, while *in situ*, to climatic wetting and drying processes. The volumetric water content (θ) of the loess was measured using twelve time domain reflectometry (TDR) probes which were calibrated for the loess prior to deployment. Soil suction and temperature were measured using twelve dielectric water potential sensors. These sensors measure the dielectric permittivity of two ceramic disks when in hydraulic equilibrium with the soil, allowing estimation of suction in the surrounding soil matrix. These sensors were selected for their field durability and measurable suction range. They are limited to measuring suctions that must be larger than 9 kPa (the air entry suction of their ceramics) and have been calibrated by the manufacturer for drying conditions only. The TDR and dielectric water potential sensors were installed at the base of individual machine augured holes that were backfilled with loess. Instruments were installed in pairs (one TDR sensor adjacent to one dielectric water potential sensor) in four horizontal arrays at depths ranging between 0.5

* Corresponding author: katherine.yates@canterbury.ac.nz

– 2.0 m below ground level (bgl). The horizontal and vertical distribution of the sensors allowed the variability of the hydraulic response across the site and progression of the wetting fronts to be examined. Rainfall precipitation was measured using a tipping bucket rain gauge with a 0.2 mm resolution. The instrumentation system was powered by one deep cycle battery charged by a solar panel. Measurements from each sensor were recorded by the data logger at ten-minute intervals from November 2017 to April 2019.

As expected, field monitoring data showed that reduction in soil suction coincide with increase in volumetric water content when rainfall percolated into the soil (Figure 1, Figure 2). Periods of drying, where soil water content decreased and suction increased, occurred as ground temperatures increased and rainfall was less frequent (summer). The greatest range in hydraulic state (θ, s) was observed < 0.5 m bgl where the soil profile was increasingly exposed to evapotranspiration, precipitation and change in air temperature and humidity. Conversely, less fluctuation was observed in the hydraulic state of loess > 1.0 m bgl across the monitored seasons. Typically, progression of the wetting front during rainfall events was limited to < 2.0 m bgl. Minimal (if any) wetting front change was observed > 2.0 m bgl for specific events. Little variation in hydraulic state was observed throughout the soil profile during winter months (May to August) when θ remained relatively high (18 – 20 %). In summer (December to February) θ reduced to 11 %.

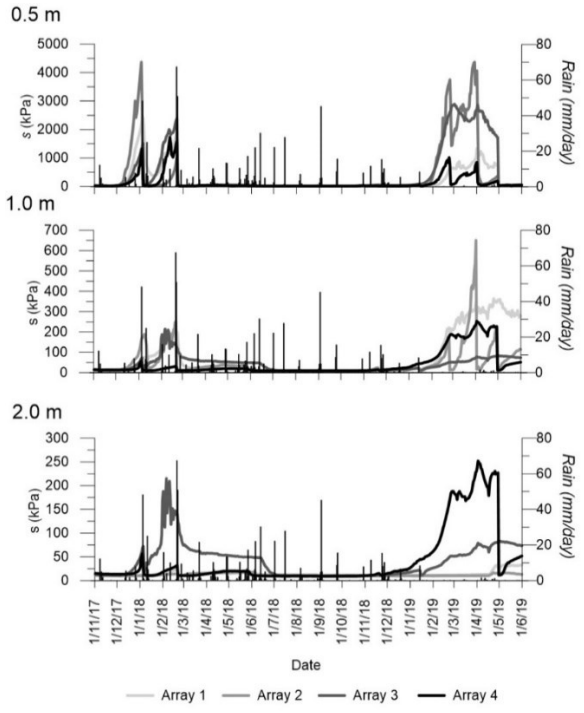

Fig. 1. Suction and daily rainfall measurements at the field instrumentation site.

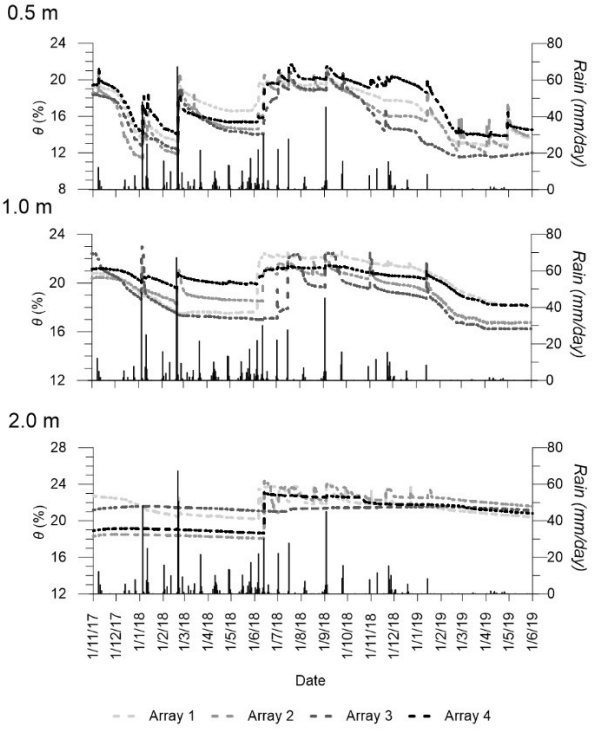

Fig. 2. Volumetric water content and daily rainfall measurements at the field instrumentation site.

3 Laboratory testing

3.1 Soil water characteristic curve

The soil-water characteristic curve (SWCC) was determined using two methods: pressure plate testing (ASTM D6836 - 16) and WP4C dewpoint potentiometer testing. Due to the low total soluble salts (TSS) measured in the loess (TSS < 0.05%) osmotic suction is negligible and matric suction and total suction may be taken as being equal. Both intact loess and recompacted loess samples were tested to determine the SWCC. Compacted samples were prepared by moist tamping to a target density range of 1.5 to 1.8 g/cm^3 which is representative of typical densities observed in Canterbury loess deposits [5]. Intact loess samples for laboratory testing were carved from larger block samples that had been hand excavated from a loess cutting near the instrumentation site.

Results from both pressure plate and dewpoint testing were combined to form the SWCC (Figure 3). Good agreement was observed between the two test methods. Linearity observed in the double logarithmic $S_r - s$ plane confirms that the SWCC, and thus the pore size distribution, can be characterised using the mathematics of fractals [12, 14]. Notably, the fractal nature allows the influence of void ratio (e) on the SWCC to be removed by normalising suction using the air entry value (s_{ae}) [15]. The s_{ae} for Akaroa loess can be related to e using:

$$s_{ae} = 30e^{-2.67} \quad (1)$$

And the air expulsion suction (s_{ex}) is defined as:

$$s_{ex} = \frac{s_{ae}}{11.3} \quad (2)$$

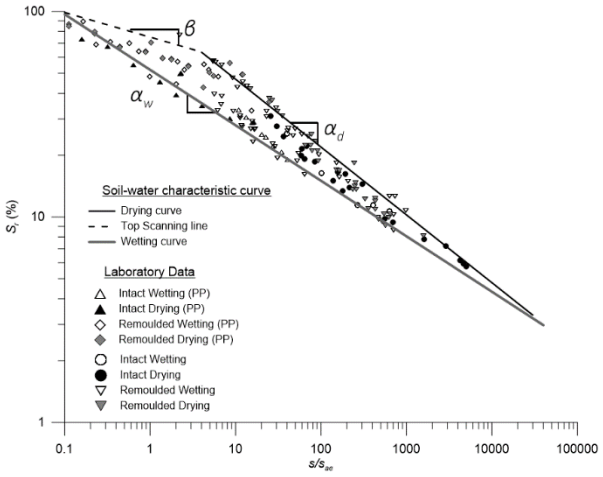

Fig. 3. Soil-water characteristic curve for intact and recompacted loess.

From Figure 3, the main drying curve of the SWCC is defined as:

$$S_r = \left(\frac{s}{s_{ae}}\right)^{-0.33} \quad (3)$$

Bounding the wetting data the main wetting curve is defined as:

$$S_r = \left(\frac{s}{s_{ex}}\right)^{-0.27} \quad (4)$$

Finally, the top scanning line is defined as:

$$S_r = \left(\frac{s}{s_{ex}}\right)^{-0.12} \quad (5)$$

In this study, the slope of the main wetting curve (α_w = -0.27) is less than that of the main drying curve (α_d = -0.33). This is unique in that for many soils, the main drying and wetting curves have the same slope in the double logarithmic $S_r - s$ plane. In practice this means that, as the loess reaches a drier hydraulic state, the scanning path required to move between the drying and wetting curves becomes shorter.

3.2 Shear strength testing

Triaxial tests were performed on both intact and recompacted samples, each approximately 50 mm in diameter and 100 mm in height. A Bishop-Wesley triaxial apparatus modified for testing saturated or unsaturated samples was used. The intact samples were hand carved out of the loess blocks. Six tests were performed on saturated samples, three intact and three recompacted, under drained conditions. Six tests were performed on unsaturated samples, three intact and three recompacted, while holding suction constant at either 200 kPa or 290 kPa. The suction was attained by subjecting the samples to drying paths from an initially saturated condition so the hydraulic states were located on the top scanning curve. Suction was applied using the axis translation technique and controlled by applying a water and air pressure differential across the sample. Another three tests were performed on unsaturated intact samples while holding the water content constant and equal to the *in situ* field value, which was approximately 2.5%. The initial suctions in these samples were measured using the WP4C device and were found to be approximately 125 MPa. The total confining stresses σ_3 used varied from 20 kPa to 150 kPa.

The variations of deviatoric stress q with axial strain ε_a are plotted in Figure 4. As expected, the stress-strain curves show an increase in maximum deviatoric stress as suction increases. Brittle responses were observed for the intact samples when suction was approximately 125 MPa. Also, when suction was 200 kPa or 290 kPa, or when saturated, the intact loess samples exhibited a tendency to strain-soften while most of the recompacted samples exhibited a tendency to strain-harden.

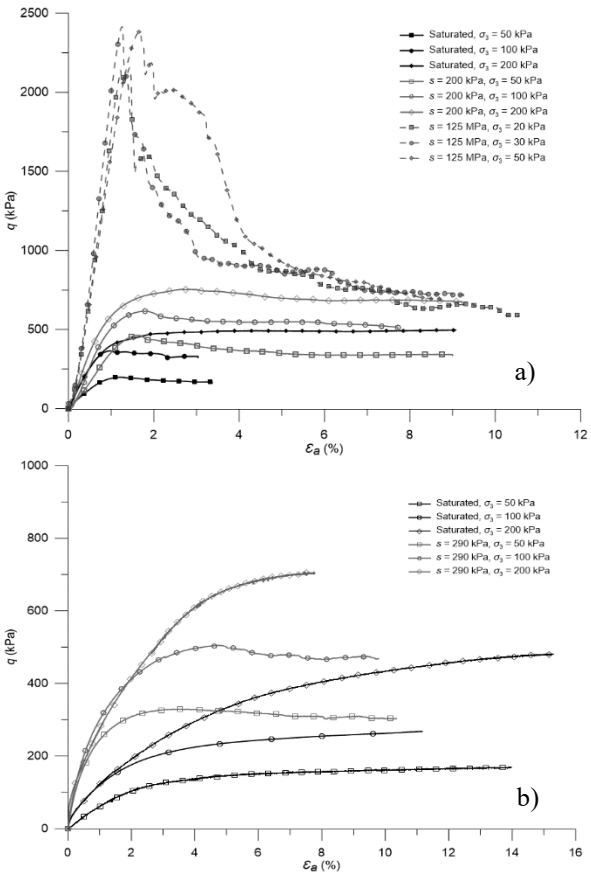

Fig. 4. (a) Triaxial stress-strain plots for saturated and unsaturated intact loess specimens; (b) Triaxial stress-strain plots for saturated and unsaturated recompacted loess specimens.

Bishop's (1959) effective stress for unsaturated soils was used to account for the contribution of suction in unsaturated triaxial testing:

$$\sigma' = (\sigma - u_a) + \chi(u_a - u_w) \quad (6)$$

where σ' is the effective stress, σ is the total stress, u_a is the pore air pressure, u_w is the pore water pressure, $s = u_a - u_w$ and χ is the effective stress parameter ($\chi = 1$ for saturated soils). The shear strength (τ) may then be approximated using:

$$\tau = c' + \sigma' \tan\varphi' = c' + \chi s \tan\varphi' + \sigma \tan\varphi' \quad (7)$$

in which φ' is the friction angle and c' is the cohesion.

The quantity $c' + \chi s \tan\varphi'$ can be treated as an equivalent cohesion, combining the true cohesion with a suction dependent component that varies in magnitude. The location of the hydraulic state on the SWCC, and thus the drying or wetting history, must be considered in the determination of χ. The relationship developed by [16] is used here when the hydraulic state is located on the main drying curve. For that case χ is determined using:

$$\chi = \left(\frac{s}{s_{ae}}\right)^{\Omega_d} \quad (8)$$

for which Ω_d = -0.55 is assumed as it is a best fit value for many soils. When the hydraulic state is located on the top scanning curve χ is determined using:

$$\chi = \left(\frac{s}{s_{ex}}\right)^{\zeta} \quad (9)$$

and when on the main wetting curve χ is determined using:

$$\chi = \left(\frac{s}{s_{ex}}\right)^{\Omega_w} \quad (10)$$

To ensure compatibility between the expressions defining the SWCC and χ the equalities $\zeta/\Omega_d = \beta/\alpha_d$, $\zeta/\Omega_w = \beta/\alpha_w$ and $\Omega_w/\Omega_d = \alpha_w/\alpha_d$ must apply [14], leading to $\Omega_w = -0.45$ and $\zeta = -0.2$. Using these relationships, the contribution of suction to the shear strength of loess was found to be adequately defined using Bishop's theory of effective stress. These data informed the derivation of peak and critical state φ' and c' values for saturated intact and remoulded specimen (Table 1).

Table 1. Peak and critical state φ' and c' values for saturated intact and remoulded specimen

Sample type	Peak	Critical state
Intact	φ' = 35 ° c' = 15 kPa	φ' = 33 ° c' = 0 kPa
Recompacted	φ' = 31 ° c' = 5 kPa	φ' = 31 ° c' = 0 kPa

The contribution of suction to the shear strength of the loess highlights the association between seasonal changes in slope stability that occurs as the *in situ* soil mass gets wetter or drier. Characterisation of the soil's mechanical response to wetting and drying can be used to inform preliminary analysis of the implications of wetting events on loess slope stability.

Discussion

3.3 Hydromechanical state of *in situ* loess

Comparison between laboratory and field data indicates that the hydraulic states of the *in situ* loess remained on scanning curves throughout the monitoring period (Figure 5). Figure 5 presents field data measured at 0.5 -1.0 m below ground level during drying periods between 6 January to 20 February in 2018, and 20 January to 22 February in 2019. These data are normalised by s_{ae} and compared with the laboratory determined SWCC. Soil density measurements of field samples were used to inform void ratios at each probe depth along the four instrumentation arrays. Data from sensors installed at 2.0 m have not been included because of the minimal variation in the hydraulic state observed in them.

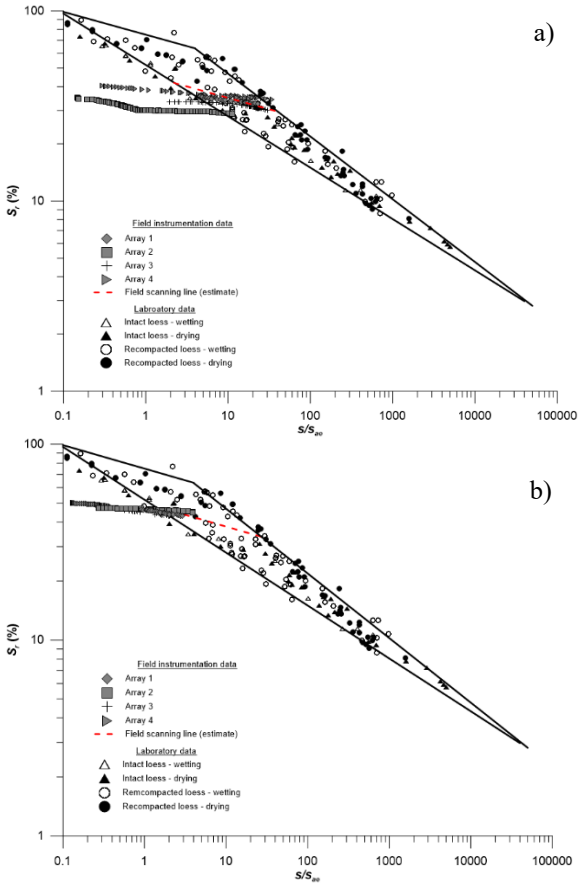

Fig. 5. Field instrumentation measurements overlaid on laboratory derived SWCC for hydraulic drying periods between (a) 6 January to 20 February 2018, and (b) 20 January to 22 February 2019

Field and laboratory data sets show that the slope of the field scanning line is the same as the slope of the top scanning curve defined from laboratory data. Furthermore, during the monitoring period, the hydraulic state of the *in situ* loess did not extend beyond the main drying curve derived in the laboratory. Conversely the field hydraulic data did travel to the left of the laboratory determined main wetting curve. Several factors may contribute to the extension of field data to left of the main wetting curve. Firstly, the influence of heterogeneity of the loess *in situ* (e.g., due to root holes and defects) may not be captured in the laboratory testing due to the small sample sizes used. Secondly, there is a possible presence of entrapped air in the *in situ* loess that is not removed by percolation of rainfall. This means that the way in which air occupies pore spaces in the field may differ from the laboratory-controlled samples. In addition, while field data measurements have been interpreted as point data, the hydraulic states the sensors measure are influenced by a large soil mass undergoing non-uniform hydraulic changes. Finally, the accuracy of the sensor calibrations during the early stages of a drying process (immediately following a wetting process) is unknown. As such, if the ceramic calibrations are invalid for wetting, then they are likely to be invalid for the initial stages of subsequent drying as the hydraulic state at the commencement of the drying has a combination of suction and volumetric water content that cannot be reliably determined.

3.4 Climatic variables and soil hydraulic change

Field instrumentation data from periods of hydraulic change has informed the approximation of climatic thresholds that give rise to wetting of this loess slope. This was achieved by temporally categorising field monitoring data into periods of hydraulic drying, wetting or no change. This allowed the corresponding climatic variables during these periods, such as rainfall intensity, rainfall duration, total rainfall, and temperature, to be observed when changes to volumetric water content and matric suction occurred (Figure 6). These data indicated that wetting was evident at the depth of the shallowest sensors (~ 0.5 m) when the average rainfall intensity (i_{av}) was > 1.5 mm/hr or the rainfall duration (D_{max}) was > 400 minutes. When i_{av} and D_{max} were below these thresholds, the distinction between wetting and drying was less clear. It was observed that i_{av} provided a clearer threshold than the maximum rainfall intensity (i_{max}) due to the natural variability rainfall intensity that is observed during a natural rainfall event. For example, during the soil wetting that occurred on 20th February 2018 (Figure 1 and 2), s reduced from > 3000 kPa to < 20 kPa at 0.5 m bgl. Correspondingly, volumetric water content (θ) increased from 12 % to 21 %. During this rainfall event the rainfall intensity peaked at 9.6 mm/hr, and averaged at 3.6 mm/hr and the maximum duration of precipitation during the wetting event was 1340 min (e.g. $i_{max} = 9.6$ mm/hr, $i_{av} = 3.6$ mm/hr, and $D_{max} = 1340$ minutes). Conversely, rainfall with the same maximum intensity i_{max} was observed between 15 March 2018 and 27 April 2018, but negligible change to s and θ was observed. This may be attributed to the shorter duration of rainfall during this period ($D_{max} = 420$ min) and a lower average rainfall intensity ($i_{av} = 1.6$ mm/hr). There was no clear threshold for total rainfall (R_T) that could be correlated to the occurrence of wetting during the monitoring period.

Wetting generally occurred when the maximum air temperature (T_{a-max}) was < 15 °C. When 25 °C > T_{a-max} > 15 °C overlap is observed between wetting and drying periods, and periods of no hydraulic change. Higher air temperatures coincided with decrease in θ and increase in s due to evapotranspiration. During these times an upward percolation of water occurred which reduced the θ and increased s at shallower depths. The θ of deeper loess did not reduce concurrently. During periods of drying some rainfall was recorded, however, a wetting front did not propagate. This may be due to evapotranspiration of water from the surface vegetation and a low unsaturated hydraulic conductivity (K_{unsat}) as s increases.

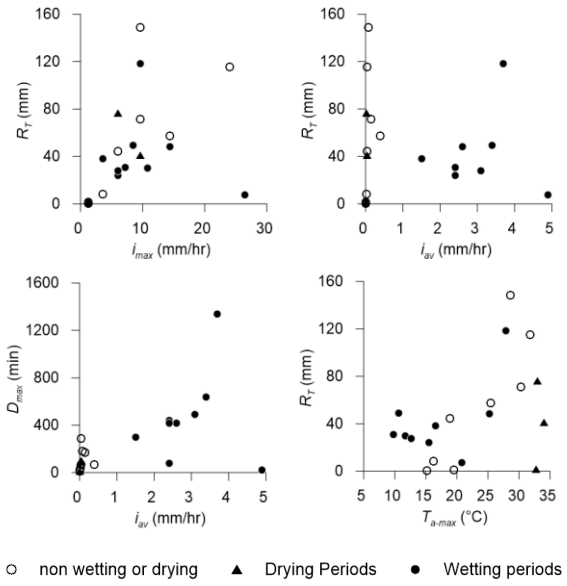

Fig. 6. Changes in hydraulic state (drying, wetting) compared with climatic variables including average rainfall intensity ($\boldsymbol{i_{av}}$), maximum rainfall intensity ($\boldsymbol{i_{max}}$), maximum rainfall duration ($\boldsymbol{D_{max}}$), total rainfall ($\boldsymbol{R_T}$), and air temperature ($\boldsymbol{T_{a-max}}$).

4 Conclusions

The unsaturated behaviour of loess from the Akaroa Harbour region, Banks Peninsula was investigated through laboratory testing and long-term monitoring of field-based instrumentation. The combination of these research methods enabled the soil-water characteristics of loess to be compared at laboratory scale and in an *in situ* loess slope. Agreement between laboratory test results of intact and recompacted loess and *in situ* loess monitoring results was observed, considering the

potential limitations of the sensors used to make the field suction measurements and soil variabilities which may be present at the field site and sensor locations. The combination of these data indicates that the *in situ* loess remained on a scanning curve for the duration of the two-year monitoring period. Change in hydraulic state of the *in situ* loess during the monitoring period highlighted the contribution of a range of climatic variables that contribute to wetting of the soil mass. It was observed that the average rainfall intensity had a stronger correlation with the occurrence of wetting than the maximum rainfall intensity. In general, wetting of the *in situ* loess occurred during rainfall events where i_{av} > 1.5 mm/hr or D_{max} > 400 minutes.

The authors would like to acknowledge the contributions of Environment Canterbury and the New Zealand Geotechnical Society, which collectively funded this project. Also, funding through the ARC Future Fellowship scheme (FT200100820) awarded to the second author is gratefully acknowledged.

References

1. E. Griffiths, *Loess of Banks Peninsula.* New Zealand J. Geol Geophys, **16** (1973)
2. D. Ives, *Nature and distribution of loess in Canterbury, New Zealand.* New Zealand J. Geol Geophys, **16** (1973)
3. J.D. Raeside, *Loess Deposits of the South Island, New Zealand, and Soils Formed on them.* New Zealand J. Geol Geophys, **7** (1964)
4. P.J. Tonkin, E. Runge, and D. Ives, *A Study of Late Pleistocene Loess Deposits, South Canterbury, New Zealand.* Quat. Res, **4** (1974)
5. K. Yates, C.H. Fenton, and D.H. Bell, *A review of the geotechnical characteristics of loess and loess-derived soils from Canterbury, South Island, New Zealand.* Eng. Geol, **236** (2018)
6. T.J. Hughes, *A Detailed Study of Banks Peninsula Loess Shear Strength*, in *Department of Geological Sciences*. MSc Eng Geol thesis. University of Canterbury. (2002)
7. T.W.D. Jowett, *An investigation of the geotechnical properties of loess from Canterbury and Marlborough*, in *Department of Geological Sciences*. MSc Eng Geol thesis. University of Canterbury (1995)
8. D.H. Bell, P.J. Glassey, and M.D. Yetton. *Chemical stabilisation of dispersive loessical soils, Banks Peninsula, Canterbury, New Zealand*. in *5th International IAEG Congress*. Buenos Aires, Argentina.(1986)
9. C.S. White, *Earthqauke induced fissuring in Banks Peninsula loessial soils: A geotechnical investigation of the Ramahana Road Fissure trace*, in *Department of Geological Sciences*. MSc Eng Geol thesis. University of Canterbury (2016)
10. T. Vo and A.R. Russell, *Stability charts for curvilinear slopes in unsaturated soils.* Soils Found, **57** 4 (2017)
11. A.R. Russell, *How water retention in fractal soils depends on particle and pore sizes, shapes, volumes and surface areas.* Geotechnique, **64** 5 (2014)
12. A.R. Russell and O. Buzzi, *A fractal basis for soil-water characteristics curves with hydraulic hysteresis (Technical Note).* Geotechnique, **62** 3 (2012)
13. H. Yang, A. Khoshghalb, and A.R. Russell, *Fractal-based estimation of hydraulic conductivity from soil–water characteristic curves considering hysteresis.* Géotechnique Lett., **4** 1 (2014)
14. T. Vo, H. Yang, and A.R. Russell, *Cohesion and suction induced hang-up in ore passes.* Int. J. Rock Mech. Min. **87** (2016)
15. K. Yates and A.R. Russell, *The unsaturated characteristics of natural loess in slopes, New Zealand.* Geotechnique, Ahead of Print (2022) https://doi.org/10.1680/jgeot.21.00042
16. N. Khalili and M.H. Khabbaz, *A unique relationship for χ for the determination of the shear strength of unsaturated soils.* Geotechnique. **48** 5 (1998)